RMetS
Royal Meteorological Society

# Serial clustering of extratropical cyclones in a multi-model ensemble of historical and future simulations

T. Economou,[a]* D. B. Stephenson,[a] J. G. Pinto,[b,c] L. C. Shaffrey[b] and G. Zappa[b]
[a]*Department of Mathematics and Computer Science, University of Exeter, UK*
[b]*Department of Meteorology, University of Reading, UK*
[c]*Institute for Geophysics and Meteorology, University of Cologne, Germany*

*Correspondence to: T. Economou. Laver, North Park Road, Exeter, EX4 4QE. E-mail: t.economou@exeter.ac.uk

**This study has investigated serial (temporal) clustering of extratropical cyclones simulated by 17 climate models participating in CMIP5. Clustering was estimated by calculating the dispersion (ratio of variance to mean) of 30 December–February counts of Atlantic storm tracks passing near each grid point. Results from single historical simulations of 1975–2005 were compared to those from historical ERA40 reanalyses from 1958 to 2001 and single future model projections of 2069–2099 under the RCP4.5 climate change scenario.**

**Models were generally able to capture the broad features in reanalyses reported previously: underdispersion/regularity (i.e. variance less than mean) in the western core of the Atlantic storm track surrounded by overdispersion/clustering (i.e. variance greater than mean) to the north and south and over Western Europe. Regression of counts onto North Atlantic Oscillation (NAO) indices revealed that much of the overdispersion in the historical reanalyses and model simulations can be accounted for by NAO variability.**

**Future changes in dispersion were generally found to be small and not consistent across models. The overdispersion statistic, for any 30-year sample, is prone to large amounts of sampling uncertainty which obscures the climate change signal. For example, the projected increase in dispersion for storm counts near London in the CNRMCM5 model is 0.1 compared to a standard deviation of 0.25. Projected changes in the mean and variance of NAO are insufficient to create changes in overdispersion that are discernible above natural sampling variations.**

*Key Words:* storm clustering; CMIP5; Poisson process; extratropical cyclones; regional climate change

*Received 22 December 2014; Revised 19 May 2015; Accepted 21 May 2015; Published online in Wiley Online Library*

## 1. Introduction

Extratropical cyclones (ETCs) pose a major societal risk in Europe, especially when they occur successively in clusters, which then leads to large aggregate losses. For example, in the recent winter of 2013/2014, numerous ETCs caused destruction of infrastructure and disruption to transport and business in Europe: windstorms *Christian*, *Xaver*, *Dirk* and *Tini* caused insured losses of $1.382, 0.961, 0.468 and 0.356 billion resulting in a total insured loss of more than $3 billion (source: http://www.perils.org; accessed 1 July 2015).

There are three main reasons why storms might cluster in time:

1. By chance – even if storm occurrences happen completely at random, some of them will occur in clusters;
2. Due to modulation by large-scale climate modes. Time-varying background climatic conditions can cause the rate of occurrence to be non-stationary (Mailier *et al.*, 2006);
3. Dependence between successive storms – e.g. a 'parent' storm might generate one or more 'offspring' (secondary cyclogenesis; Parker, 1998).

Previous studies have used Poisson process concepts to investigate temporal clustering of storms using observations and reanalyses data. For historical windstorms affecting the North Atlantic and Europe, Mailier *et al.* (2006) have found that there is more clustering than can be expected by chance at both flanks and downstream areas of the main North Atlantic storm track. Moreover, evidence was provided that more extreme storms cluster to a greater extent (Vitolo *et al.*, 2009). Using a different tracking methodology, Pinto *et al.* (2013) confirmed that the identified spatial pattern of clustering and its intensification for more severe storms is a robust feature in reanalysis data.

Mailier *et al.* (2006) also showed that clustering can be largely explained by modulation of storm counts by large-scale climate modes. A large part of the contribution from the large-scale modes to the storm clustering derives from the modulation of the eddy-driven jet over the North Atlantic. Indeed, the occurrence of historical storm series affecting Western Europe is related to a recurrent extension of an intensified eddy-driven jet towards Western Europe for periods of one or more weeks (Pinto *et al.*, 2014). Moreover, upstream cyclone development (secondary cyclogenesis; Parker, 1998) is strongly related to

cyclone clustering, leading to the development of multiple cyclones on a single jet streak (Pinto *et al.*, 2014).

Kvamstø *et al.* (2008) showed that a simulation from a general circulation model (GCM) underestimated clustering compared to reanalysis and failed to capture the relationship between clustering and modes of climate variability. Large differences between three GCM simulations and reanalysis were also noted in Mailier (2007, chapter 6) who also found that differences in model responses prohibited conclusive statements about the future. Pinto *et al.* (2013) investigated future changes in clustering using an ensemble of 20 runs from a single GCM and found evidence, based on the ensemble mean, pointing to a possible decrease in cyclone clustering over parts of the Northern Atlantic and Western Europe, particularly north of 50°N. Note however that Pinto *et al.* (2013) also found evidence of considerable sampling variability, between ensemble members, in estimates of clustering statistics (their Figure 6). This implies that such estimates based on relatively short time periods (e.g. 30 years) might be quite uncertain which in turn has an effect on the uncertainty regarding future changes of such statistics. This is investigated in detail later, in section 3.3.

This study provides a first investigation of clustering of North Atlantic extratropical cyclones and its future changes using a large ensemble of climate models. Simulations from 17 different models computed for the recent fifth phase of the Coupled Model Inter-comparison Project (CMIP5) multi-model experiment are considered (Taylor *et al.*, 2012). The following questions are addressed:

1. How well do the CMIP5 climate models capture the clustering seen in historical reanalyses?
2. How does clustering change in future climate model projections and how model-dependent is the response?
3. Can the changes be understood in terms of changes in physical drivers such as the North Atlantic Oscillation (NAO) or are they simply due to natural variability in storm counts?

Section 2 provides a brief description of the tracking algorithm used to produce cyclone tracks from CMIP5 and reanalysis data, and how the NAO was defined and calculated. Section 3 shows results from quantifying clustering in historical and future model simulations but also reanalyses. In addition, a simple statistical model is implemented to investigate variation and future changes in clustering in terms of the NAO. Section 4 gives the conclusions and a discussion of the results.

## 2. Data

### 2.1. Storm tracks from reanalyses

Objective feature-identification software (Hodges, 1994) was used to extract ETC tracks from 6-hourly ECMWF reanalysis (ERA40) data, for the period December 1958 to November 2001, i.e. 43 historical winters. Individual cyclone tracks were identified by tracking local maxima in relative vorticity at 850 hPa just above the boundary layer (about 1.5 km above sea level).

Cyclone tracks are defined as 6-hourly measurements of cyclone intensity and location in winters December–February (DJF). Minimum sea-level pressure (MSLP) is taken here as the intensity measure used to define extreme storms and, for extremes, note that MSLP is strongly related to other variables such as wind speed (Figure 2 in Economou *et al.*, 2014). A region defined by (90°W, 25°E) and (30°N, 70°N) is discretised using a 2.5° × 2.5° grid, and at each grid point a 6.3° (700 km) radius circle is considered following the approach of Pinto *et al.* (2013). This choice of radius is within the range of effective radius for extratropical cyclones (600–1000 km; Rudeva and Gulev, 2007) and corresponds to a plateau of quasi-constant values of a particular dispersion statistic (section 2.4) over most of the study area (Pinto *et al.*, 2013, their Figure S1). To avoid problems with multiple counting, only the highest intensity event is counted for each track passing through the circle.

### 2.2. Model-simulated storm tracks

CMIP5 is a comprehensive collection of experiments in which many climate modelling groups around the globe produced a suite of past and future climate simulations (Taylor *et al.*, 2012). The tracking algorithm described above was then used to extract storm tracks for 17 CMIP5 models (Zappa *et al.*, 2013a) based on simulations of 30 historical DJF winters (December 1975 to February 2005) and 30 future DJF winters (December 2069 to February 2099). The future simulations used the RCP4.5 forcing scenario which gives around 2 °C global mean warming by 2100 (IPCC, 2013).

CMIP5 models manage to adequately capture the number of North Atlantic and European cyclones in winter, however on average they simulate a too zonal storm track, with too many cyclones propagating into Europe and too few in the Norwegian Sea area (Zappa *et al.*, 2013a). Nevertheless, some of the CMIP5 models have a realistic representation of the North Atlantic storm track location and cyclone intensity compared to reanalysis data. Under climate change, the number of cyclones is projected to decrease in the Mediterranean and Norwegian Sea areas, but to slightly increase over the UK (Sansom *et al.*, 2013; Zappa *et al.*, 2013b). This response seems to be only weakly affected by the model biases in the location of the storm track, giving confidence to the model projections (Zappa *et al.*, 2013b).

For some models there are multiple simulations for each period, based on different model initialisations, however here only a single simulation is considered per model –thus avoiding the problem of having to compare results from models with different numbers of runs. This is also more comparable to the real world where there is only one realisation in the past and future periods. For illustration, Figure 1 shows time series of storm counts from ERA40 and CNRMCM5 (National Centre for Meteorological Research, France) for a grid point near London (1.25°W, 51.25°N). The mean storm count for ERA40 is slightly lower than the one from the historical period in CNRMCM5 but overall the model counts show similar behaviour to the reanalysis counts. The mean storm count appears to slightly increase in the future at this location – this is consistent with Zappa *et al.* (2013b) and Sansom *et al.* (2013) who found a slight tendency for an increase in the number of extratropical cyclones in the multi-model mean of CMIP5 future projections.

### 2.3. NAO indices

The NAO index has been shown to be a major driver in ETC clustering (Mailier *et al.*, 2006; Seierstad *et al.*, 2007). The fifth IPCC assessment of ETCs (Christensen *et al.*, 2014, section 14.5.1) reports that the mean NAO is likely to increase slightly in the future whereas the variance shows little change (IPCC AR5, Ch. 14, Figure 14.16a). It is therefore of interest to investigate whether the projected changes in NAO can explain changes in clustering and this is investigated here using a simple statistical model (section 3).

Observed values of the NAO index matching the ERA40 reanalysis tracks were taken from the National Oceanic and Atmospheric Administration (NOAA) webpage (http://www.noaa.gov; accessed 1 July 2015). The index is defined as the difference between sea-level pressure (SLP) in Iceland and the Azores, and is standardised to have zero mean and unit variance. For CMIP5 runs, an index was calculated by subtracting the mean SLP based on an 1861–1900 climatology, over a region north of 55°N, and between 90°W and 60°E from the mean SLP over a region between 20 and 55°N and between 90°W and 60°E (Gillett and Fyfe, 2013). The NAO index was then calculated by standardising using the sample variance in the historical period 1975–2005.

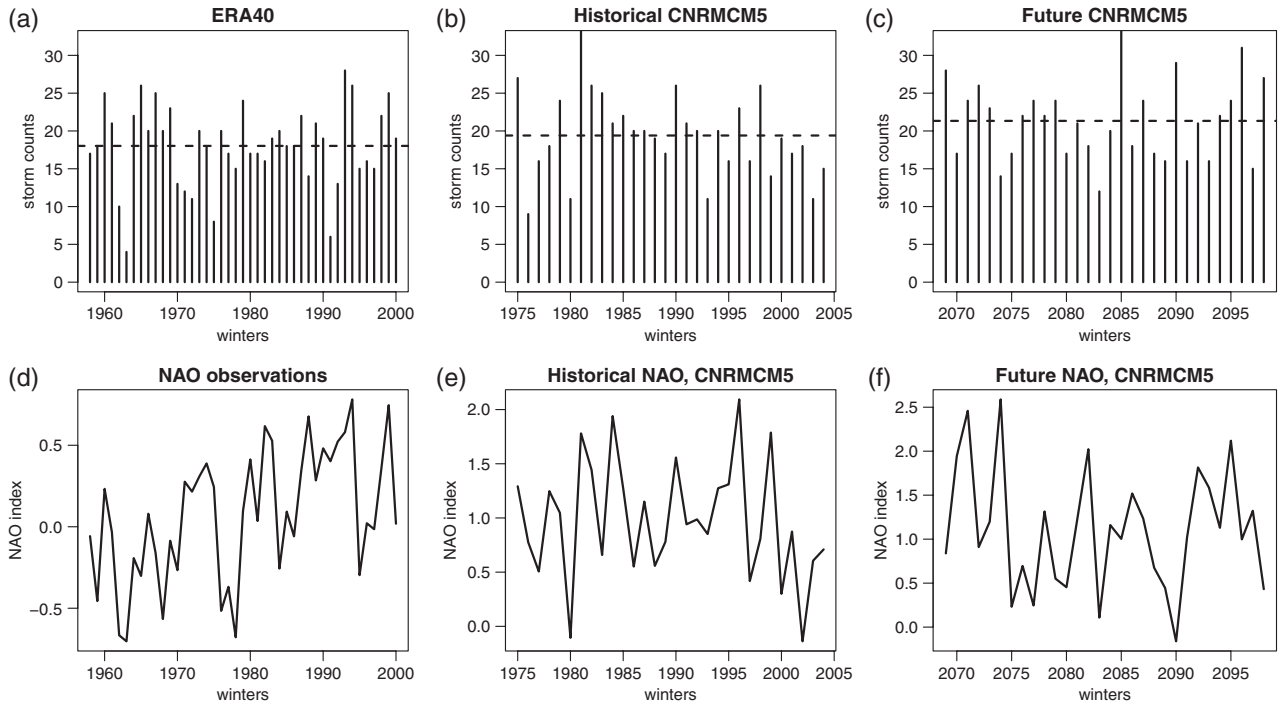


**Figure 1.** (a, b, c) Storm counts and (d, e, f) NAO indices for (a,d) reanalysis/observations, (b,e) historical simulation from CNRMCM5, and (c,f) future simulation from CNRMCM5. Horizontal dashed lines indicate the mean storm count.

### 2.4. *Dispersion of counts as a measure of clustering*

If storms were to occur completely at random, then the simplest model to describe this is the homogeneous Poisson process with constant intensity $\lambda$ (Cox and Isham, 1980), which implies that the number of events in any time interval of length $T$ is Poisson distributed with mean $\mu = \lambda T$ and variance $\sigma^2 = \lambda T$. Here, $T$ is the winter period December–February. Deviations from this process can give rise to events that either appear more clustered or more regular. The number of events per unit time is then either overdispersed ($\sigma^2 > \mu$) or underdispersed ($\sigma^2 < \mu$) (Mailier *et al.*, 2006).

Let $Y$ be the number of storms passing through a region in a winter. A dispersion measure $\phi = Var(Y)/\mathbb{E}[Y] - 1$ can be estimated by $s_y^2/\bar{y} - 1$, where $s_y^2$ is the sample variance of $Y$. Positive (negative) values of $\phi$ suggest clustering (regularity) whereas $\phi = 0$ suggests complete serial randomness.

Mailier *et al.* (2006) showed that a large fraction of overdispersion over Europe (in reanalysis data) can be captured by characterising the mean of $Y$ as a function of climate indices such as the NAO. More recently, Blender *et al.* (2015) have used a Weibull renewal process to also quantify clustering in ERA-Interim reanalyses, and have confirmed high clustering (overdispersion) over Europe and Scandinavia.

Extreme storms at a grid point are defined as ones whose MSLP value went below a threshold, specifically the 0.2 empirical quantile based on all MSLP minima associated with storms at that grid point. The thresholds are different for historical and future projections to allow for the fact that the distribution of storm intensity or the background MSLP might change (Chang, 2014).

## 3. Results

In what follows, letters 'H' and 'F' are used to refer to statistics from either the 30 historical or the 30 future winters from each climate simulation.

### 3.1. *Historical clustering*

Figure 2 shows dispersion in historical runs of each CMIP5 model and the ERA40 reanalysis, as well as the multi-model mean. The models qualitatively capture the gross features seen in ERA-40 reanalysis: regularity along the storm track axis (the upper-tropospheric jet axes are indicated on all plots for reference) and clustering around the edges of the track. These features are also consistent with previous clustering studies (Mailier *et al.*, 2006; Vitolo *et al.*, 2009; Pinto *et al.*, 2013). Figure 3 shows estimates of $\phi_H$ but for extreme storms. Again, models largely capture the overall features seen in ERA40 reanalysis: $\phi$ increases everywhere, and the overdispersion becomes particularly large over Northern Europe, Scandinavia and the Azores. This increase in dispersion for more extreme storms was previously noted for reanalysis in Vitolo *et al.* (2009) and Pinto *et al.* (2013). Notice however that the models tend to underestimate the dispersion statistic over the UK/Central Europe, something that is consistent with a zonal North Atlantic jet simulated by the CMIP5 models, which is associated with a too strong and southward displaced jet over Central Europe compared to reanalysis data (Figure 9a in Zappa *et al.*, 2013a).

There is considerable spread in the dispersion statistic across the individual CMIP5 models, with some models showing a large overestimation of cyclone clustering compared to the ERA40. It is unlikely that this spread is simply explained in terms of particular modelling choices such as resolution. For example, models IPSL-CM5A-LR and IPSL-CM5A-MR, which only differ in the resolution of the atmospheric component, show a relatively similar level of cyclone clustering as measured by the dispersion statistic. In a similar manner, low-resolution models (grid spacing of about 300 km) exhibit either quite large (e.g. MIROC-ESM) or small (e.g. BCC-CSM1_1) values of the dispersion statistic. Furthermore, no clear association is found between cyclone clustering and the climatological model biases in the storm track position noted in Zappa *et al.* (2013a). For example, among the models that strongly overestimate cyclone clustering compared to ERA40 (Figure 2), three of them have a southward displaced North Atlantic storm track (MIROC-ESM, MIROC-ESM-CHEM and CSIRO-MK360) and two of them have a too zonal storm track into Europe (IPSL-CM5A-LR and IPSL-CM5A-MR) according to the classification given in Zappa *et al.* (2013a). This suggests that other processes, such as biases in the representation of large-scale atmospheric variability (section 3.3.2) or secondary cyclogenesis, need to be taken into account to explain cyclone clustering in the individual models. Lastly, as shown later in section 3.3.2, there

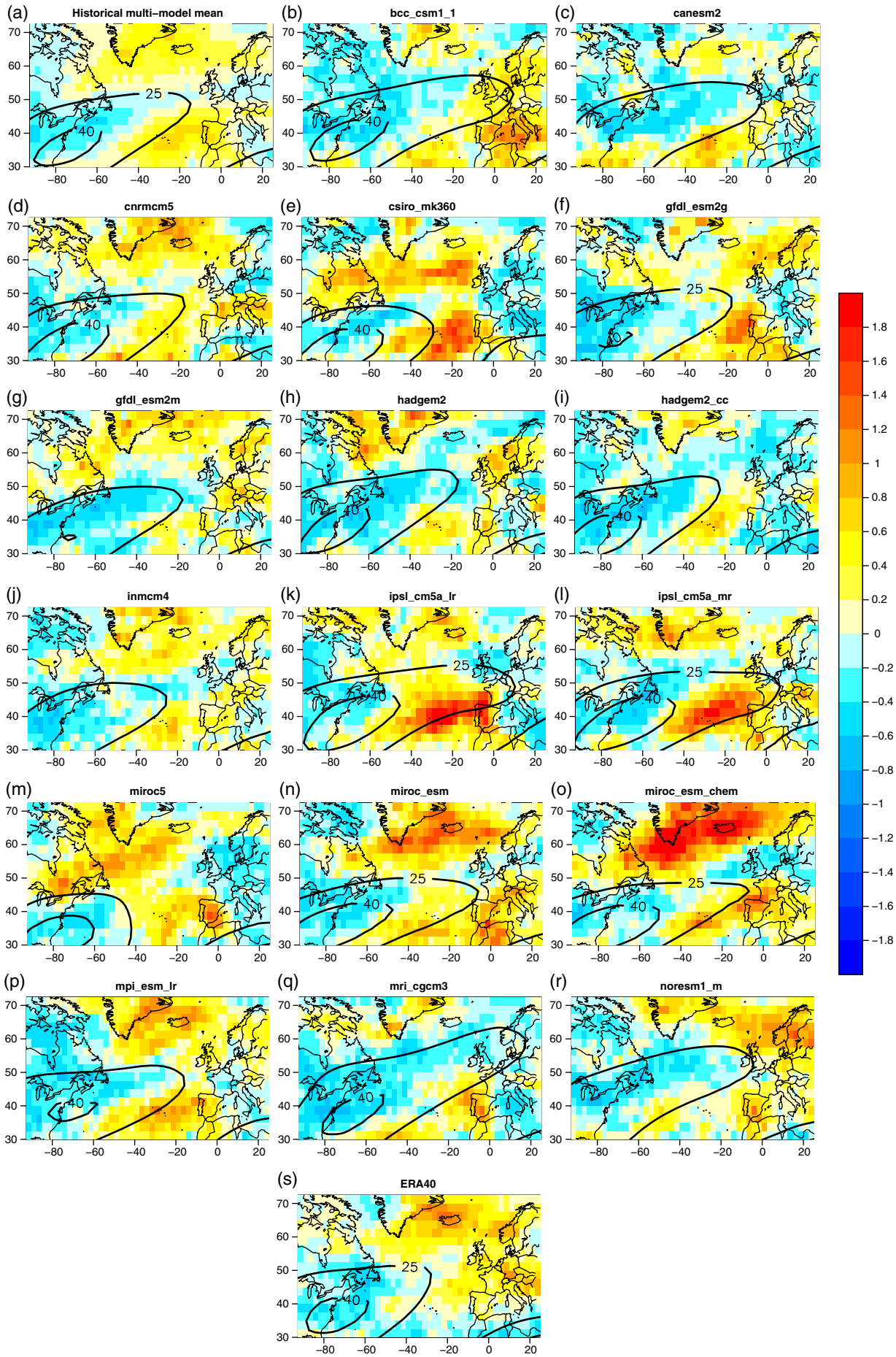


**Figure 2.** Maps of dispersion statistic $\phi_H$. Top left panel is the multi-model mean, followed by each model in alphabetical order from left to right. The bottom middle panel shows ERA40. The upper tropospheric jet axis is indicated by contours (25 and 40 m s$^{-1}$) of the mean zonal wind at 250 hPa for each model.

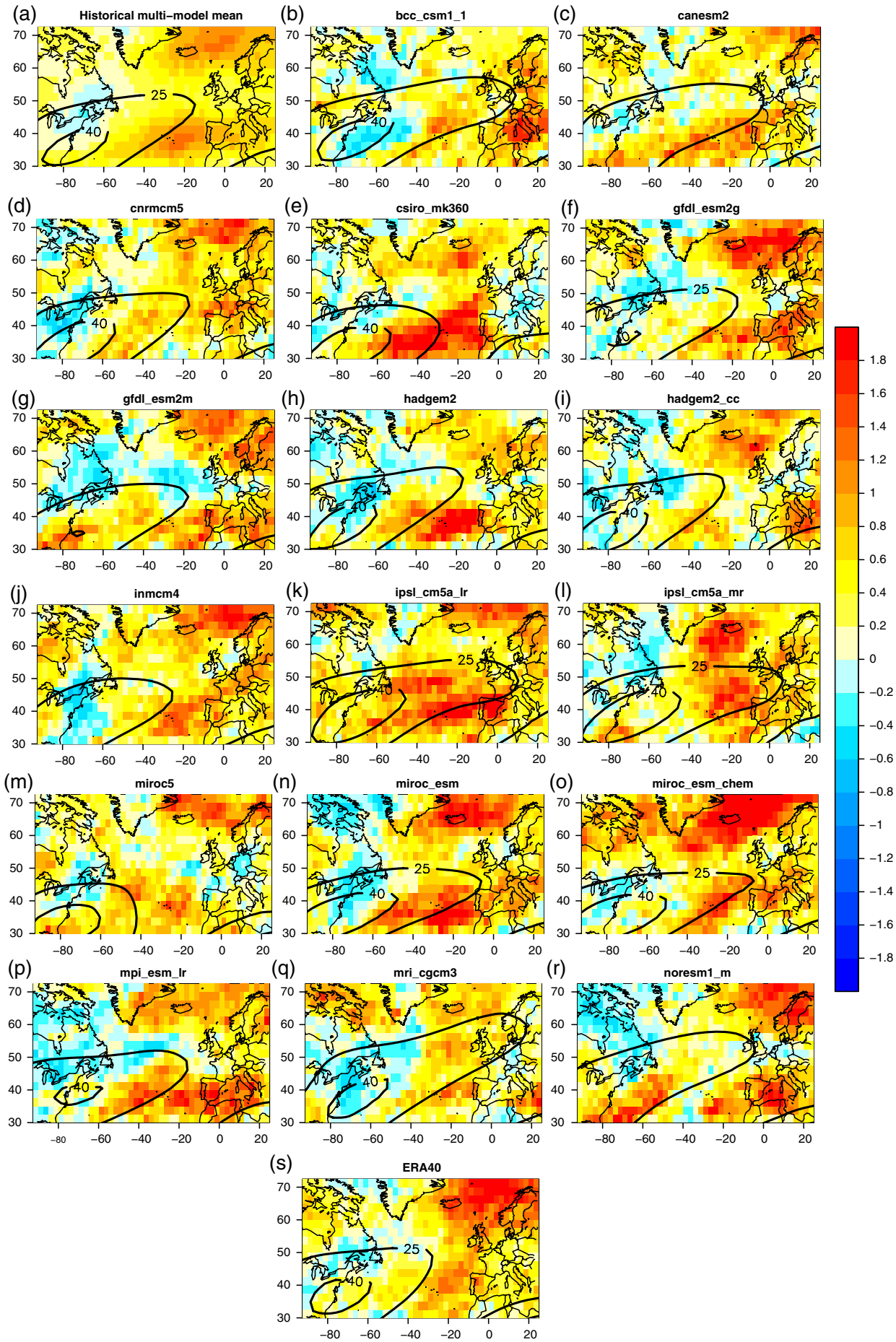


**Figure 3.** Maps of dispersion statistic $\phi_H$ for extreme storms. Top left panel is the multi-model mean, followed by each model in alphabetical order from left to right. The bottom middle panel shows ERA-40.

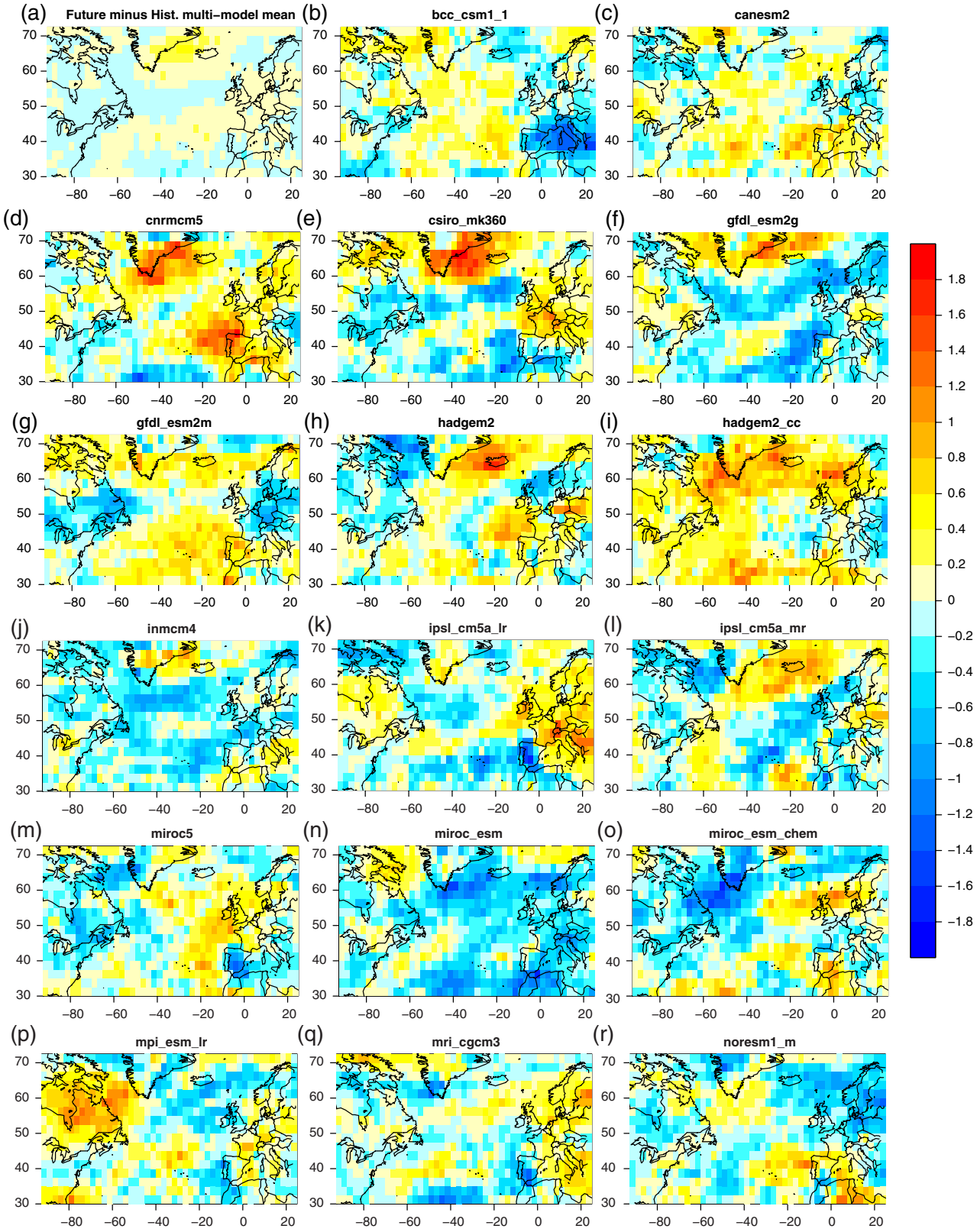


**Figure 4.** Maps of projected changes in dispersion $\Delta\phi = \phi_F - \phi_H$. Top left panel is the multi-model mean, followed by each model in alphabetical order from left to right.

is substantial sampling uncertainty in estimating the dispersion statistic from short (30-year) records, implying that models with similar characteristics might exhibit different storm clustering behaviour.

### 3.2. *Future projections*

Figure 4 shows estimates of changes in dispersion $\Delta\phi = \phi_F - \phi_H$. There is considerable variation with little agreement between models. However, the multi-model mean (upper left panel but also more clearly in Figure 5a) shows a similar response to the ensemble mean of ECHAM5 GCM simulations in Figure 5e of Pinto *et al.* (2013): i.e. increase in underdispersion over the region of cyclone genesis and an increase of overdispersion south of the storm track.

Figure 5(b) shows multi-model mean $\Delta\phi$ estimates for extreme storms (again there is substantial variability between models and the multi-panel plot is given in Figure S1). The multi-model mean plot shows increase in dispersion near Greenland and over Northern Europe which is different from the ensemble mean of ECHAM5 in Figure 5f of Pinto *et al.* (2013), who detect a decrease in dispersion over the same areas. This may be attributed to the

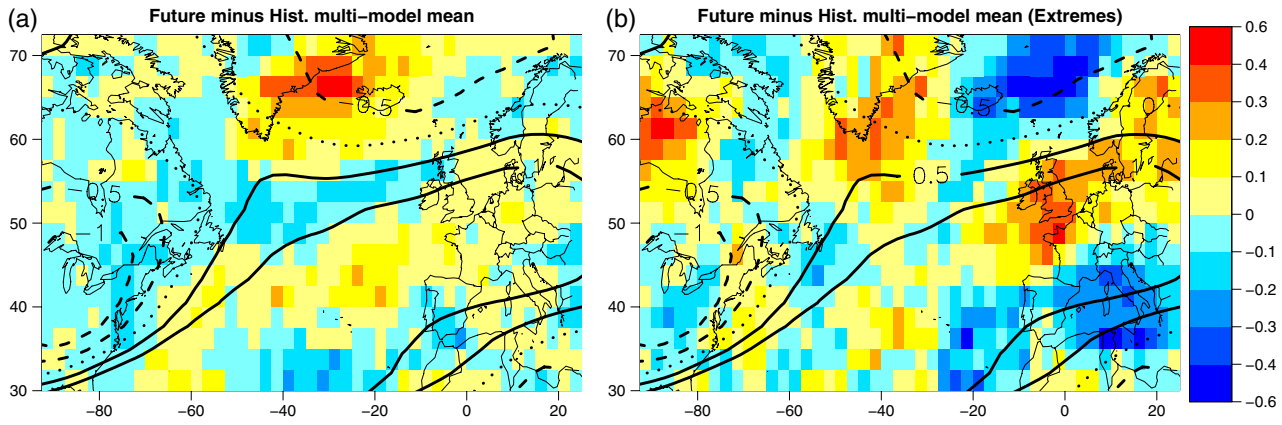


**Figure 5.** Maps of multi-model means of projected changes in dispersion $\Delta\phi = \phi_F - \phi_H$ for (a) all storms and (b) extreme storms. Contours of multi-model mean jet changes are indicated at $-1$, $-0.5$, 0, 0.5 and 1 m s$^{-1}$, using dashed, dotted and solid lines for negative, zero and positive values respectively.

following reasons: (i) different GCM, in this case ECHAM5, (ii) different cyclone tracking methodology, and (iii) the definition of extreme storms. Pinto *et al.* (2013) use background pressure to calculate local thresholds whereas we use a threshold based on the lowest MSLP measurement of each storm that went through a grid point. Therefore the extremes here are relative to the maximum intensity of all other storms within the neighbourhood, as calculated by the tracking algorithm – so results regarding the extremes may not be comparable to ones created by other tracking algorithms. Multi-model means are not very informative with respect to an actual prediction of the future, especially if the variability about these means is quite large, as is apparent from Figure 4.

To test the sensitivity of the multi-model mean to potentially outlying models, the analysis was repeated but ignoring the following models: HADGEM2, HADGEM2_cc, CANESM2, MRI_CGCM3 and NORESM1_M. These five models were chosen due to their qualitative deviation from ERA-40 dispersion in Figure 2. The associated multi-model mean maps of projected changes were effectively the same as Figure 5, suggesting the means are robust to individual model discrepancies.

Note that all of the above analyses were repeated using the more severe RCP8.5 scenario but the results are not shown for conciseness. The main findings regarding future changes were that: (1) as with RCP4.5, there was considerable variability between the models, (2) there was very little qualitative agreement when comparing future changes from RCP4.5 and RCP8.5 maps of individual models and (3) the multi-model mean plot of $\Delta\phi$ for the two scenarios was qualitatively similar but with RCP8.5 changes being more pronounced. Point 2 indicates that much of the individual model responses is dominated by internal climate variability. This will be investigated in the next section.

### 3.3. *Understanding the changes*

#### 3.3.1. *Are changes in dispersion due to changes in the mean counts?*

Changes in $\phi = s^2/\bar{y} - 1$ are either due to changes in the sample mean $\bar{y}$ or the sample variance $s^2$ of the counts, or both. To investigate this, we recalculated $\Delta\phi$ in two different ways: (i) assuming $\bar{y}$ remains the same in the future so that $\Delta\phi = \left(s_F^2 - s_H^2\right)/\bar{y}_H$ shown in Figure S2 and (ii) assuming the variance remains the same so that $\Delta\phi = s_H^2\left[1/\bar{y}_F - 1/\bar{y}_H\right]$ shown in Figure S3. Comparing Figures S2 and S3 with Figure 4, it is evident that changes in dispersion are mostly driven by changes in the variance of the counts. The same holds for extreme storms (not shown for brevity).

#### 3.3.2. *Why did the variance of the counts change?*

For count data, it can be shown by Taylor expansion (Appendix A) that $4Var\left(\sqrt{Y}\right) \approx Var\,(Y)\,/\mathbb{E}[Y]$ (Anscombe, 1948; Yu, 2009). The square root is a variance-stabilising transformation (i.e. such that variance is unaffected by changes in mean) and if the data are over- or underdispersed, the variance of $\sqrt{Y}$ will be larger/smaller than 1/4, implying that the dispersion measure can be approximated by $\phi \approx 4Var\left(\sqrt{Y}\right) - 1$ and estimated by $4s^2_{\sqrt{Y}} - 1$ where $s^2_{\sqrt{Y}}$ is the sample variance of $\sqrt{Y}$. Figure 6 shows a scatter plot of $s^2_y/\bar{y} - 1$ versus and $4s^2_{\sqrt{Y}} - 1$ based on ERA40 counts at each grid point. The plot indicates that the approximation is good, except for a handful of points that are located near the edge of the map where storm counts are zero for most winters. This approximation to $\phi$ is now used to build a simple statistical model to characterise $\sqrt{Y}$ and thus clustering.

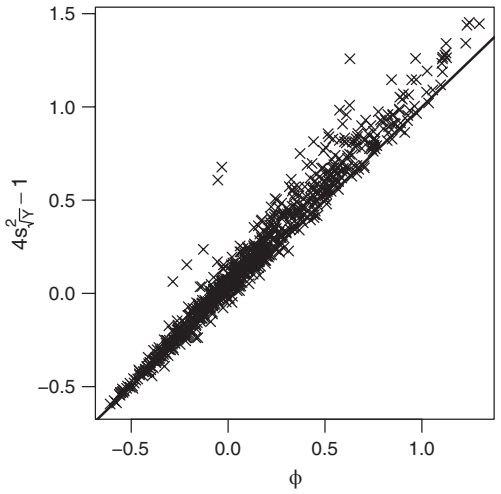


**Figure 6.** Plot of dispersion statistic $\phi$ and its approximation $4s^2_{\sqrt{Y}} - 1$ for ERA-40 reanalysis. Each cross corresponds to a grid point.

As a simple model for the relationship between $\sqrt{Y}$ and the NAO, we consider

$$\sqrt{Y} = \alpha + \beta X + \epsilon \qquad (1)$$

where $X$ is the seasonal mean NAO index and $\epsilon$ is independent normally distributed noise. To test the assumption of a linear relationship between $\sqrt{Y}$ and $X$, we actually considered a more general model where $\sqrt{Y} = \alpha + f(X)$ and $f(\cdot)$ is a smooth (possibly nonlinear) function and $\epsilon \sim N(0, \tau^2)$. This is a Generalised Additive Model (GAM) which was implemented in R (R Core Team, 2014) using the 'mgcv' package (Wood, 2006, gives details). The model was fitted at each grid point and CMIP5 model, and Figure 7 shows the fit for ERA40 and CNRMCM5 at the grid cell near London and another cell near Scotland (8.75°W, 58.75°N). Model CNRMCM5 was chosen as it closely matched ERA40 clustering in Figure 2. There is little evidence supporting a nonlinear relationship and this is true for most model/grid cell

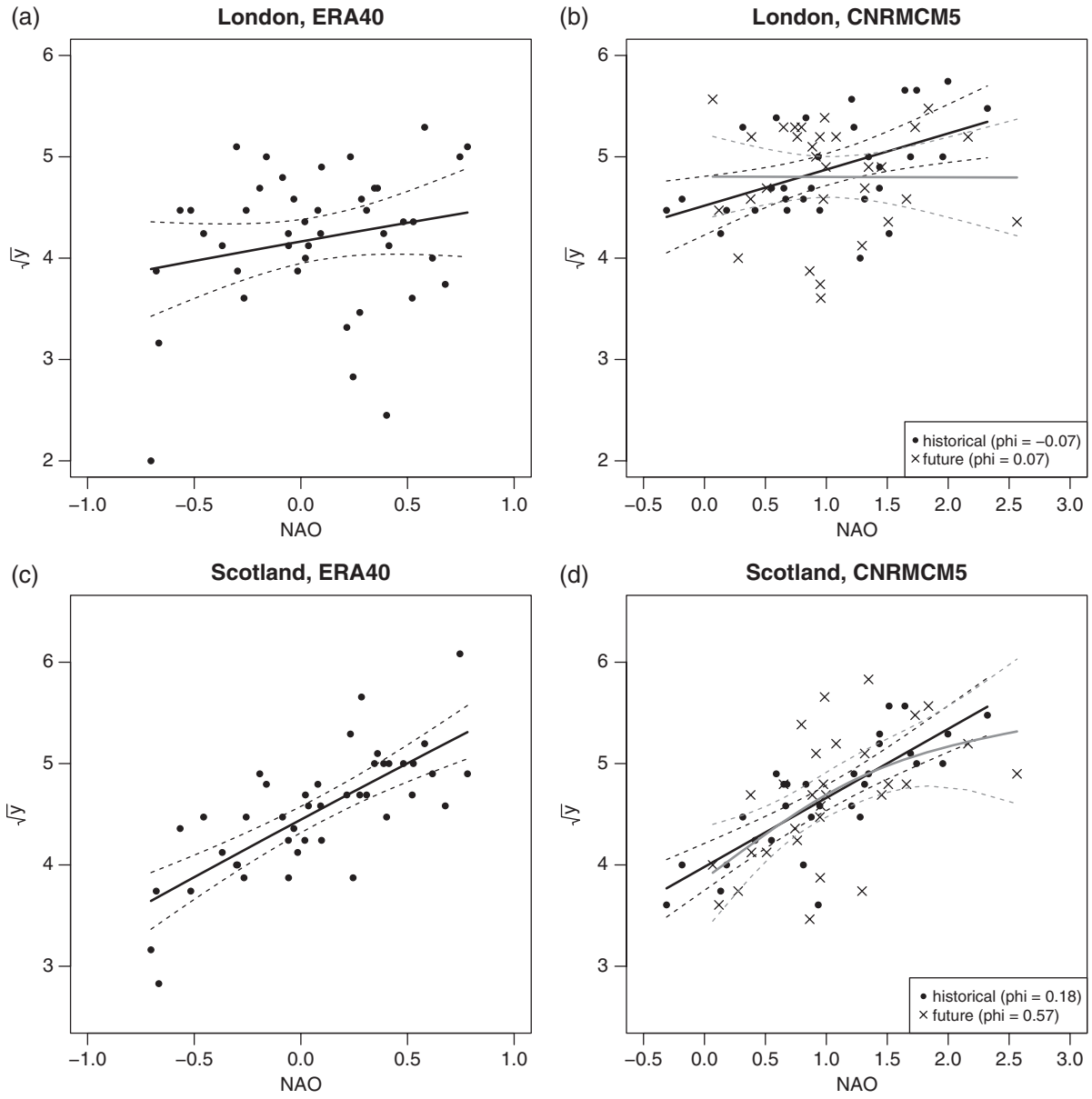


**Figure 7.** Estimated relationship between square root of counts and NAO with associated 95% confidence intervals, for counts (a,b) near London and (c,d) in Scotland. Black (grey) lines correspond to historical (future) data. (a,c) relates to ERA40 reanalysis and (b,d) to CNRMCM5. The legend in (b,d) shows historical and future estimates of the dispersion statistic $\phi$.

combinations investigated (not shown for brevity). Note that, although Figure 7(c) suggests a nonlinear relationship, the width of the confidence bands is large enough so that a linear relationship cannot be confidently rejected. The relationship between NAO and $\sqrt{Y}$ is stronger in Scotland, implying that NAO explains more of the clustering than it does near London (see also map in Figure 8). Furthermore, the CNRMCM5 plots indicate a change in the relationship between $\sqrt{Y}$ and NAO, however it is clear from the 95% confidence intervals that there is no significant difference in the historical and future curves.

Equation (1) can be shown to imply (Appendix B)

$$\phi \approx 4Var\left(\sqrt{Y}\right) - 1 = 4\beta^2 Var\,(X) + 4Var\,(\epsilon) - 1. \quad (2)$$

The dispersion is simply the sum of two parts due to the variability of NAO and the variance of the error term $\epsilon$. The error term accounts for influential factors other than the NAO as well as the random variations in $\sqrt{Y}$. To investigate the effect of NAO variability on clustering, Figure 8 shows maps of $4\widehat{\beta}^2_{\mathrm{H}} s^2_{X_{\mathrm{H}}}$, i.e. the estimate of the first part of Eq. (2), for the historical period (based on historical estimates of $\beta$ and $Var\,(X)$). Comparing this with the original $\phi$ estimates in Figure 2, it is evident that a large proportion of the historical (and also future but not shown) patterns can be attributed to NAO variability – in particular the overdispersion north and south of the storm track. So now the question is whether future changes in NAO are the major driver behind the apparent changes in storm clustering.

Assuming the relationship between storm counts and NAO remains the same in the future (i.e. $\alpha$ and $\beta$ unchanged), Eq. (2) implies that the changes in clustering are approximately given by

$$\begin{aligned}\Delta\phi = {} & 4\beta^2 \{Var\,(X)_{\mathrm{F}} - Var\,(X)_{\mathrm{H}}\} \\ & + 4\{Var\,(\epsilon)_{\mathrm{F}} - Var\,(\epsilon)_{\mathrm{H}}\}. \end{aligned} \quad (3)$$

In other words, changes in clustering are driven by changes in the variability of NAO and also by changes in the variance of $\epsilon$. The estimate of the first term in Eq. (3), i.e. the change in NAO variance, is plotted in Figure 9 (based on estimates of $\beta$ from historical data). This is rather different to Figure 4, which depicts $\Delta\phi$ estimates, implying that changes in NAO explain little of the changes in clustering. The term $Var\,(X)_{\mathrm{F}} - Var\,(X)_{\mathrm{H}}$ is very small (which is in agreement with the IPCC findings) and the changes are dominated by the $\{Var\,(\epsilon)_{\mathrm{F}} - Var\,(\epsilon)_{\mathrm{H}}\}$ term. So although the NAO explains much of the clustering, future changes are dominated by changes in the variance of $\epsilon$, i.e. random variations not related to NAO.

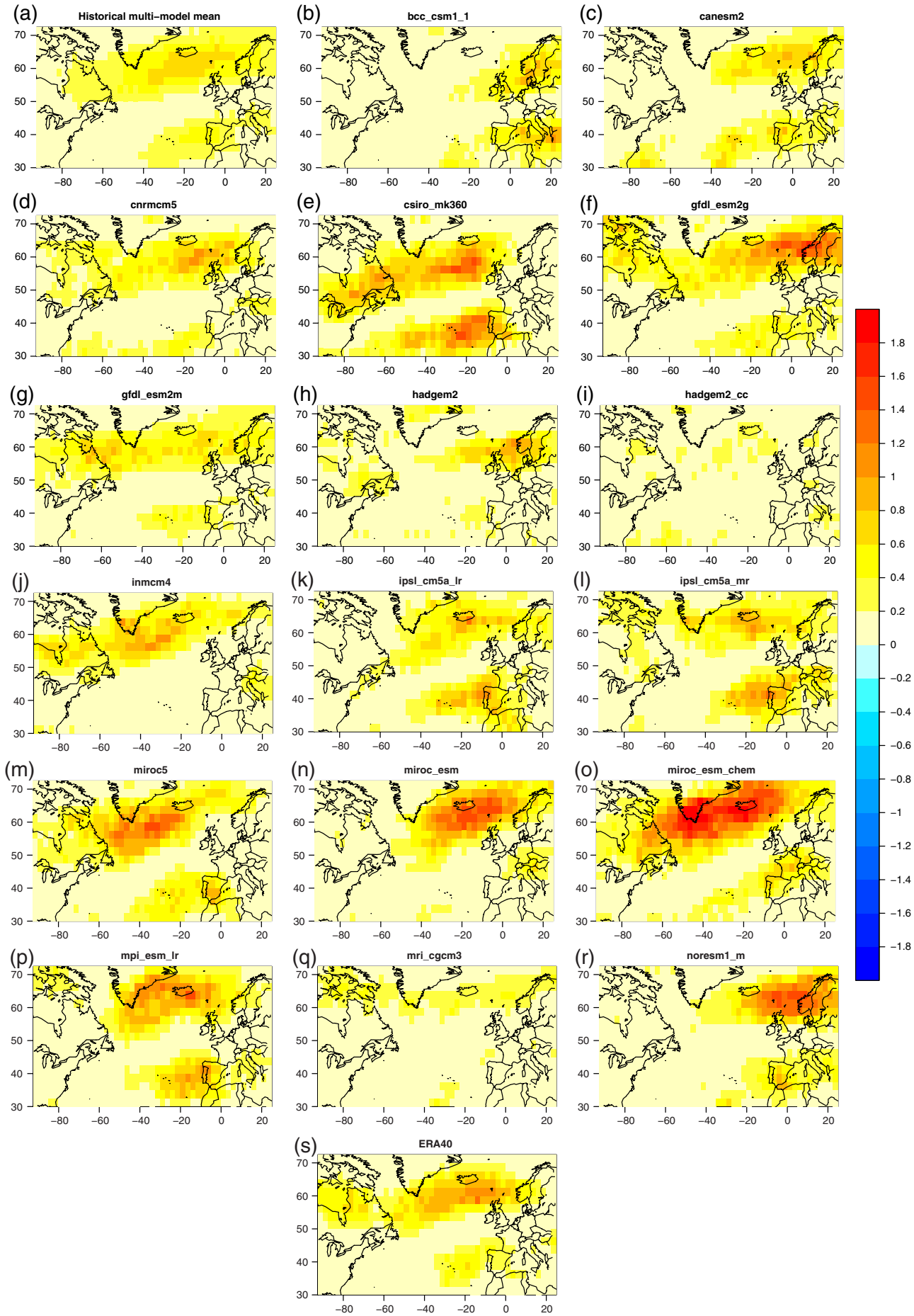


**Figure 8.** Estimates of $4\beta^2 Var\,(X)$ for the historical data. Top left panel is the multi-model mean, followed by each model in alphabetical order from left to right. The bottom middle panel shows ERA40.

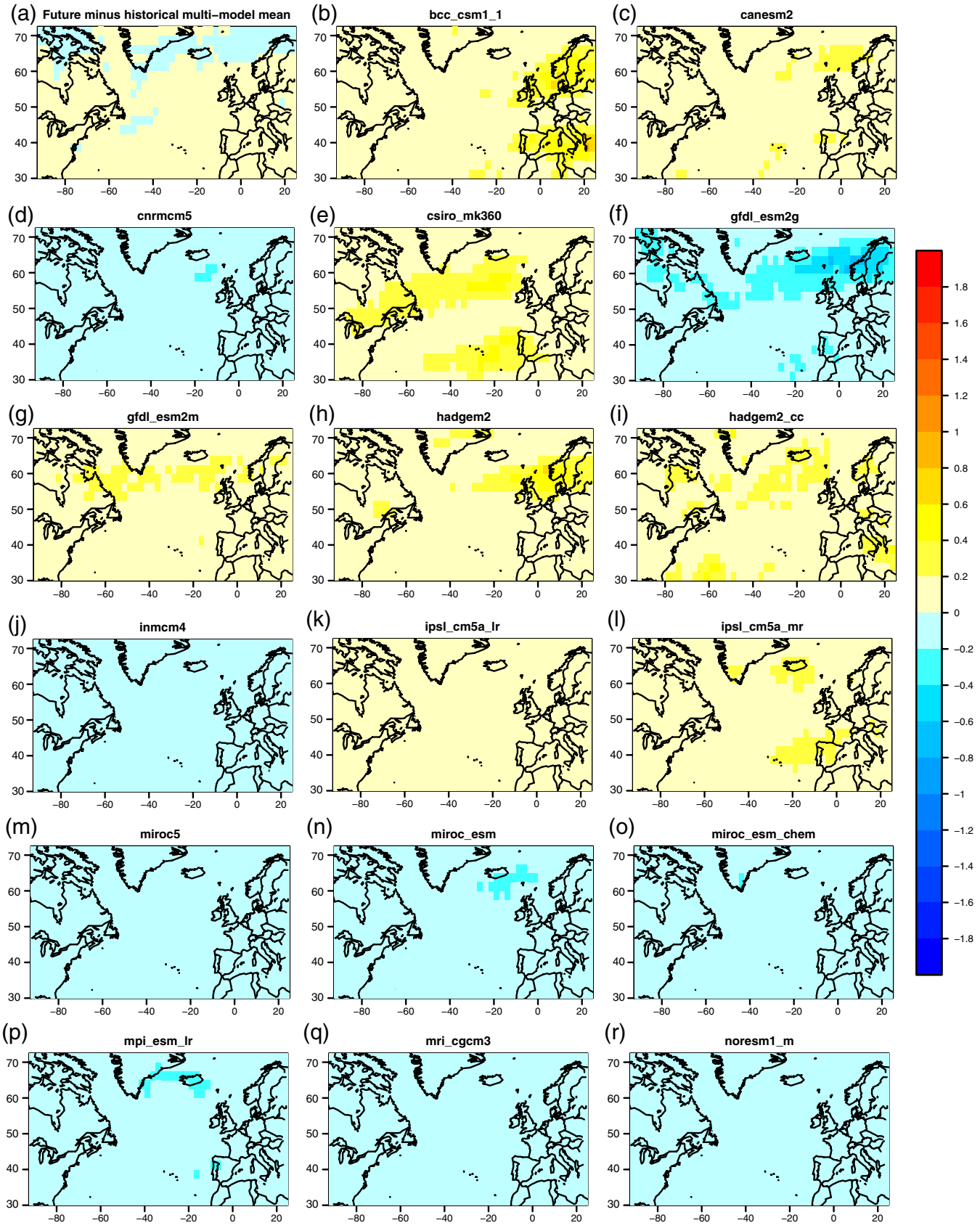


**Figure 9.** Estimates of $4\beta^2\left(Var\,(X)_{\mathrm{F}} - Var\,(X)_{\mathrm{H}}\right)$. Top left panel is the multi-model mean, followed by each model in alphabetical order from left to right.

Future changes in $\phi$ are explained by non-NAO-related variations in $\sqrt{Y}$. Simulation experiments are now used to show that these changes can be explained by natural variation in the year to year counts. Considering the London grid point again, the clustering measure $\phi$ increased from $-0.07$ to 0.07 in the future for CNRMCM5. Model (1) was fitted to the historical data and then 1000 stochastic simulations of the square root of storm counts for the 30-year historical period were produced, calculating the estimate of $\phi$ each time. These 1000 samples were used to produce a histogram of the sampling distribution of estimated $\phi$, shown in Figure 10(a). The apparent increase in dispersion would be hard to detect because of the large variance of the distribution, which is essentially due to the large natural interannual variability in the counts. The same simulation experiment was performed, this time forcing NAO to be fixed in each 30-year period (i.e. $Var\,(X) = 0$), and the resulting histogram of $\phi$ is shown in

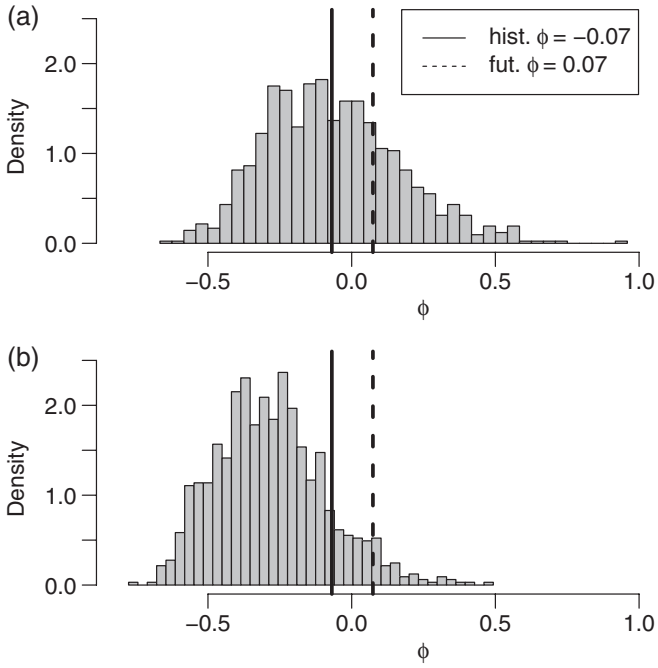


**Figure 10.** (a) Histogram showing the sampling distribution of the dispersion statistic $\phi$ near London for CNRMCM5. (b) is as (a) but assuming the variance of NAO is zero over the 30-year historical period. The vertical lines show the historical (solid) and future (dashed) $\phi$ estimates.

Figure 10(b). The distribution shifted to the left since the variance of the square root counts is smaller (since $Var\,(X) = 0$), thus producing a more regular process. The plot shows that even with NAO fixed, there is a large amount of uncertainty in estimating $\phi$ from short records of 30 winters. The standard deviation in the $\phi$ estimates for London are 0.25 and 0.2 for NAO random and NAO fixed respectively – much larger than the change of 0.1 in $\phi$.

## 4. Conclusions

This study has investigated serial (temporal) clustering of extra-tropical cyclones simulated by 17 climate models participating in CMIP5. Dispersion of track counts from single historical simulations of 1975–2005 were compared to those from historical reanalyses from 1958-2001 ERA-40 and single future model projections of 2069–2099 under the RCP4.5 scenario. Our main findings are that:

- Models qualitatively capture the broad features reported in reanalyses: underdispersion/regularity (i.e. variance less than mean) in the western core of the Atlantic storm track surrounded by overdispersion/clustering (i.e. variance greater than mean) to the north and south and over Western Europe. Furthermore, models are also able to capture the increase in overdispersion noted for more extreme storms in the reanalyses;
- Much (but not all) of the overdispersion in the historical reanalyses and the 17 model simulations can be accounted for by NAO variability. Track counts on the non-western edges of the main Atlantic storm track have strong monotonic dependency on NAO and so variations in NAO lead to additional variance in counts (overdispersion);
- Future changes in dispersion were generally found to be small and not consistent across models. The multi-model mean response resembles the single-model ensemble mean response discussed in Pinto *et al.* (2013). The equivalent multi-model mean dispersion for more extreme storms suggests that, on average, clustering of extreme storms increases over Northern Europe and Scandinavia in the RCP4.5 scenario;
- The 30-year overdispersion statistic is prone to large amounts of sampling uncertainty that obscures the climate change signal. For example, the projected increase in dispersion for storm counts near London in the CNRMCM5 model is 0.1 compared to a standard deviation of 0.25. Projected changes in the mean and variance of NAO are insufficient to create changes in overdispersion that are discernible above natural sampling variations. Hence, one should not expect to see the multi-model ensemble mean response in future observations.

It is worth mentioning that, while the NAO variability can explain the occurrence of cyclone clustering over the North Atlantic basin, it does not explain all of the variability over Europe (Figure 8). European windstorm occurrence is related to the occurrence of an extended and intensified jet towards Europe (e.g. Hanley and Caballero, 2012; Gómara *et al.*, 2014) and hence may have an effect upon clustering; Figure 2 shows where the jet stream core area corresponds to the areas with underdispersion in the western North Atlantic and also the ERA-40 map in Figure 2 where overdispersion is evident on both flanks and downstream of the North Atlantic jet, where the variance of the jet is enhanced. As such, jet stream biases in CMIP5 models Zappa *et al.* (2013a) may explain the biases in clustering noted in Figure 2. Moreover, Pinto *et al.* (2014) have recently provided evidence that a recurrent extension of an intensified eddy-driven jet towards Western Europe lasting at least 1 week is one of the main factors leading to the occurrence of historical storm series.

The jet stream is projected to intensify and extend towards Europe under future climate conditions (e.g. Figure 5(a)). These changes may have implications for storm clustering –for example the increase in clustering over Central Europe for extreme cyclones in Figure 5(b). Future studies are required to determine the relative role of jet stream changes to the possible changes in clustering in CMIP5 models, and in how far other mechanisms (like secondary cyclogenesis) play a more important role.

Lastly, among the possible reasons identified for the differences between CMIP5 models in how they capture clustering were potential biases in large-scale atmospheric variability and secondary cyclogenesis. A detailed analysis of the impacts of both of these on cyclone clustering in the individual models is left for future work.

## Acknowledgements

This research was supported by NERC project CREDIBLE. We thank Nathan Gillett for kindly providing the NAO indices for the CMIP5 models. We also thank Kevin Hodges for providing ERA40 cyclone tracks and Phil Sansom for valuable input.

## Supporting information

The following supporting information is available as part of the online article:
**Figure S1.** Multi-model mean and individual model changes in dispersion statistic for extreme storms.
**Figure S2.** Projected dispersion changes assuming no change in mean storm counts.
**Figure S3.** Projected dispersion changes assuming no change in variance of storm counts.

## Appendix A

### Square root transformation of counts

Consider the random variable $Y$ with mean $\lambda$ and variance $Var\,(Y)$. Let $T(Y)$ be a transformation where $T()$ is the square root. If $T(Y)$ is expanded about $\mu$ using Taylor series (Yu, 2009)

then $T(Y) = T(\mu) + T'(\mu)(Y - \mu) + o(Y - \mu)$ which gives

$$\sqrt{Y} \approx \sqrt{\mu} + \frac{1}{2}\left(\frac{Y}{\sqrt{\mu}} - \sqrt{\mu}\right),$$

which implies

$$Var\left(\sqrt{Y}\right) \approx \frac{1}{4}\frac{Var\,(Y)}{\mu},$$

so that $4Var\left(\sqrt{Y}\right) \approx Var\,(Y)/\mu$. The approximation breaks down for very small values of the mean $\mu$.

## Appendix B

### Linear model for $\sqrt{Y}$

The square root stabilizes the variance (makes it constant) so that the linear model $\sqrt{Y} = \alpha + \beta X + \epsilon$ where $\epsilon \sim N(0, \sigma^2)$ in Eq. (1) becomes plausible –i.e. a model where the mean is separable from the variance. Then under this model,

$$\begin{aligned} Var\left(\sqrt{Y}\right) &= Var\,(\alpha) + Var\,(\beta X) + Var\,(\epsilon) \\ &= \beta^2 Var\,(X) + \sigma^2, \end{aligned}$$

giving rise to Eq. (2).

## References


Anscombe FJ. 1948. The transformation of Poisson, binomial and negative binomial data. *Biometrika* **35**: 246–254, doi: 10.1093/biomet/35.3-4.246.short.

Blender R, Raible CC, Lunkeit F. 2015. Non-exponential return time distributions for vorticity extremes explained by fractional poisson processes. *Q. J. R. Meteorol. Soc.* **141**: 249–257, doi: 10.1002/qj.2354.

Chang EKM. 2014. Impacts of background field removal on CMIP5 projected changes in Pacific winter cyclone activity. *J. Geophys. Res.: Atmos.* **118**: 4626–4639, doi: 10.1002/2013JD020746.

Christensen JH, Krishna Kumar K, Aldrian E, An SI, Cavalcanti IFA, de Castro M, Dong W, Goswami P, Hall A, Kanyanga JK, Kitoh A, Kossin J, Lau NC, Renwick J, Stephenson DB, Xie SP, Zhou T. 2014. Climate phenomena and their relevance for future regional climate change. In *Climate Change 2013: The Physical Science Basis. Contribution of Working Group I to the Fifth Assessment Report of the Intergovernmental Panel on Climate Change*, Stocker TF, Qin D, Plattner GK, Tignor M, Allen SK, Boschung J, Nauels A, Xia Y, Bex V, Midgley PM. (eds.): 1217–1308. Cambridge University Press: Cambridge, UK and New York, NY.

Cox DR, Isham V. 1980. *Stochastic Processes*, *Monographs on Statistics and Applied Probability*. Chapman & Hall/CRC: London.

Economou T, Stephenson DB, Ferro CAT. 2014. Spatio-temporal modelling of extreme storms. *Ann. Appl. Stat.* **8**: 2223–2246, doi: 10.1214/14-AOAS766.

Gillett NP, Fyfe JC. 2013. Annular mode changes in the CMIP5 simulations. *Geophys. Res. Lett.* **40**: 1189–1193, doi: 10.1002/grl.50249.

Gómara I, Pinto JG, Woollings T, Masato G, Zurita-Gotor P, Rodríguez-Fonseca B. 2014. Rossby wave-breaking analysis of explosive cyclones in the Euro-Atlantic sector. *Q. J. R. Meteorol. Soc.* **140**: 738–753, doi: 10.1002/qj.2190.

Hanley J, Caballero R. 2012. The role of large-scale atmospheric flow and Rossby wave breaking in the evolution of extreme windstorms over Europe. *Geophys. Res. Lett.* **39**: L21708, doi: 10.1029/2012GL053408.

Hodges K. 1994. A general method for tracking analysis and its application to meteorological data. *Mon. Weather Rev.* **122**: 2573–2585.

IPCC. 2013. *Climate Change 2013: The Physical Science Basis. Contribution of Working Group I to the Fifth Assessment Report of the Intergovernmental Panel on Climate Change*, Stocker TF, Qin D, Plattner GK, Tignor M, Allen SK, Boschung J, Nauels A, Xia Y, Bex V, Midgley PM. (eds.). Cambridge University Press: Cambridge, UK and New York, NY, 1–1535, doi: 10.1017/CBO9781107415324.

Kvamstø NG, Song Y, Seierstad IA, Sorteberg A, Stephenson DB. 2008. Clustering of cyclones in the ARPEGE general circulation model. *Tellus A* **60**: 547–556, doi: 10.1111/j.1600-0870.2008.00307.x.

Mailier PJ. 2007. 'Serial clustering of extratropical cyclones', PhD thesis. University of Reading: Reading, UK.

Mailier PJ, Stephenson DB, Ferro CAT, Hodges KI. 2006. Serial clustering of extratropical cyclones. *Mon. Weather Rev.* **134**: 2224–2240.

Parker DJ. 1998. Secondary frontal waves in the north Atlantic region: A dynamical perspective of current ideas. *Q. J. R. Meteorol. Soc.* **124**: 829–856.

Pinto JG, Bellenbaum N, Karremann MK, Della-Marta PM. 2013. Serial clustering of extratropical cyclones over the North Atlantic and Europe under recent and future climate conditions. *J. Geophys. Res.: Atmos.* **118**: 12 476–12 485, doi: 10.1002/2013JD020564.

Pinto JG, Gómara I, Masato G, Dacre HF, Woollings T, Caballero R. 2014. Large-scale dynamics associated with clustering of extratropical cyclones affecting Western Europe. *J. Geophys. Res.: Atmos.* **119**: 13704–13719, doi: 10.1002/2014JD022305.

R Core Team. 2014. *R: A Language and Environment for Statistical Computing*. http://www.R-project.org/ (accessed 1 July 2015).

Rudeva I, Gulev SK. 2007. Climatology of cyclone size characteristics and their changes during the cyclone life cycle. *Mon. Weather Rev.* **135**: 2568–2587.

Sansom PG, Stephenson DB, Ferro CAT, Zappa G, Shaffrey L. 2013. Simple uncertainty frameworks for selecting weighting schemes and interpreting multimodel ensemble climate change experiments. *J. Clim.* **26**: 4017–4037, doi: 10.1175/JCLI-D-12-00462.1.

Seierstad IA, Stephenson DB, Kvamstø NG. 2007. How useful are teleconnection patterns for explaining variability in extratropical storminess? *Tellus A* **59**: 170–181, doi: 10.1111/j.1600-0870.2007.00226.x.

Taylor KE, Stouffer RJ, Meehl GA. 2012. An overview of CMIP5 and the experimental design. *Bull. Am. Meteorol. Soc.* **93**: 485–498.

Vitolo R, Stephenson DB, Cook IM, Mitchell-Wallace K. 2009. Serial clustering of intense European storms. *Meteorol. Z.* **18**: 411–424, doi: 10.1127/0941-2948/2009/0393.

Wood SN. 2006. *Generalized Additive Models, an Introduction with R*. Chapman & Hall/CRC: London.

Yu G. 2009. Variance stabilizing transformations of Poisson, binomial and negative binomial distributions. *Stat. Probab. Lett.* **79**: 1621–1629, doi: 10.1016/j.spl.2009.04.010.

Zappa G, Shaffrey LC, Hodges KI. 2013a. The ability of CMIP5 models to simulate north Atlantic extratropical cyclones. *J. Clim.* **26**: 5379–5396.

Zappa G, Shaffrey LC, Hodges KI, Sansom PG, Stephenson DB. 2013b. A multimodel assessment of future projections of North Atlantic and European extratropical cyclones in the CMIP5 climate models. *J. Clim.* **26**: 5846–5862.


 